NASA TN D-1301

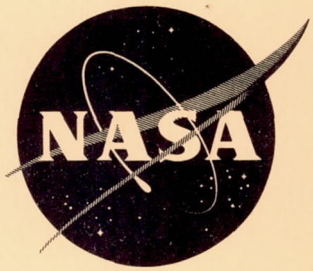

TECHNICAL NOTE

D-1301

AERODYNAMIC CHARACTERISTICS OF A 4-FOOT-DIAMETER DUCTED FAN MOUNTED ON THE TIP OF A SEMISPAN WING

By Kenneth W. Mort and Paul F. Yaggy

Ames Research Center
Moffett Field, Calif.

NATIONAL AERONAUTICS AND SPACE ADMINISTRATION
WASHINGTON
April 1962

NATIONAL AERONAUTICS AND SPACE ADMINISTRATION

TECHNICAL NOTE D-1301

AERODYNAMIC CHARACTERISTICS OF A 4-FOOT-DIAMETER DUCTED FAN MOUNTED ON THE TIP OF A SEMISPAN WING

By Kenneth W. Mort and Paul F. Yaggy

SUMMARY

Power, free-stream velocity, and duct angle of attack were varied at several wing angles of attack to define the aerodynamic characteristics of the ducted fan, wing, and of the ducted fan and wing together.

At large duct angles of attack the inside of the upstream duct lip stalled causing a rapid change in the duct pitching moments and an accompanying increase in the power required. At low horizontal velocities this lip stall would probably limit the rate of descent of a vehicle with a wing-tip-mounted ducted fan.

During low-speed, level, unaccelerated flight (30 to 80 knots) it appeared that a vehicle, with a configuration similar to that examined, would require less power if it were supported by a wing and ducted fans than if it were supported only by ducted fans.

INTRODUCTION

Tests of a wing-tip-mounted 4-foot-diameter ducted fan have been made for a limited range of operating conditions and the results reported in references 1 and 2. Tests at a smaller scale have been reported in references 3 and 4. The results in reference 1 are primarily for level unaccelerated flight; the present report contains data for the same model over a wider range of operating conditions.

The test objectives were: (1) to define the aerodynamic characteristics of the ducted fan and of the ducted fan and wing together for forward velocities up to about 100 knots; (2) to define the onset of any duct lip stall which might occur; (3) to determine the descent limitations imposed by duct lip stall on a vehicle employing wing-tip-mounted ducted fans; and (4) to determine the extent to which the wing reduced the power required for a representative level, unaccelerated VTOL transition program at constant forward velocities from 0 to 80 knots.

NOTATION

b	fan blade chord, in.
$\bar{c}$	wing mean aerodynamic chord, ft
c_d	duct chord, ft
C_D	total drag coefficient, $\frac{\text{drag}}{qS}$
C_{D_d}	ducted fan drag coefficient, $\frac{\text{ducted fan drag}}{qd_e c_d}$
c_{l_i}	blade-section design lift coefficient, $\frac{\text{section design lift}}{qb}$
C_L	total lift coefficient, $\frac{\text{lift}}{qS}$
C_{L_d}	ducted fan lift coefficient, $\frac{\text{ducted fan lift}}{qd_e c_d}$
C_m	total pitching-moment coefficient, $\frac{\text{pitching moment}}{qS\bar{c}}$
C_{m_d}	$\frac{\text{ducted fan pitching moment}}{qd_e c_d^2}$
C_{m_t}	$\frac{\text{ducted fan pitching moment}}{\rho n^2 d^5}$
C_N	ducted fan normal-force coefficient, $\frac{\text{ducted fan normal force}}{\rho n^2 d^4}$
C_P	ducted fan power coefficient, $\frac{\text{power}}{\rho n^3 d^5}$
C_T	ducted fan thrust coefficient, $\frac{\text{ducted fan thrust}}{\rho n^2 d^4}$
d	fan diameter, ft
d_e	duct exit diameter, ft
h	fan-blade thickness, in.
J	propeller advance ratio, $\frac{V_\infty}{nd}$

n	fan rotational speed, rps
q	free-stream dynamic pressure, lb/ft^2
r	radial distance from duct center line, ft
R	fan radius, ft
S	wing area, ft^2
SHP	shaft horsepower
V_∞	free-stream velocity, knots or fps
X	chordwise distance from duct leading edge, positive aft, in.
α_d	duct angle of attack, deg
α_w	wing angle of attack, deg
β	fan blade angle measured at tip (unless otherwise noted), deg
η	propulsive efficiency, $\frac{C_T J}{C_P} 100$, percent
ρ	density

MODEL AND APPARATUS

General Characteristics

The ducted fan studied in the present investigation and in reference 1 was an exact duplicate of those used on the Doak VZ-4DA airplane. The semispan wing panel upon which the duct was mounted had the same geometric dimensions as the left wing panel of that airplane. The general arrangement of the ducted fan and wing mounted in the wind tunnel for testing is shown in figure 1. Ducted fan and wing dimensions are shown in figure 2 and in tables I and II. As may be seen in these figures, a reflection plane was attached to the inboard end of the wing at the longitudinal plane of symmetry. All structure exposed to the air stream below this plane was isolated from the force measuring system; that is, only forces and moments on the ducted fan, wing, and reflection plane were recorded.

Fan and Inlet Guide Vanes

The eight-bladed fan had a fixed blade pitch and was tested at blade angles of 15° and 23° measured at the tip. The blades were of solid glass fiber construction. The clearance between the fan tip and the duct was approximately 0.030 inch. Blade plan-form curves are shown in figure 3; other pertinent dimensions are shown in table I.

The model was tested with seven inlet guide vanes positioned radially. These vanes were set at 0° incidence with respect to the duct axis. Pertinent characteristics and dimensions of the vanes are shown in table I.

Stators

Nine stators were used in the duct aft of the fan to remove rotation from the exit flow. Eight of the stators had 6-inch-chord NACA 0008.4 airfoil shapes superposed on an NACA a = 0.4 mean line. The ninth vane, which housed the fan drive shaft, had a 9-inch-chord NACA 0017 airfoil shape on the same mean line. Other characteristics of the stators are given in table I.

Fan Drive System

The fan was driven by a 1000-horsepower electric motor through a shaft within the wing. The motor speed could be continuously varied from 0 to 6600 revolutions per minute. Power input to the motor was recorded on a polyphase wattmeter. These readings were corrected for motor efficiency.

Instrumentation

Forces and moments on the ducted fan and wing combination were measured on the wind-tunnel six-component balance. Strain gages on the duct trunnion support tube measured the ducted fan thrust, normal force, and pitching moment.

TESTS

The wing was tested with the ducted fan removed and the end of the wing sealed. These tests consisted in varying the wing angle of attack for several free-stream velocities.

The remainder of the testing was conducted on the complete model and consisted in varying the duct angle for various wing angles and advance ratios.

REDUCTION OF DATA

Duct Trunnion Strain-Gage Data

The thrust gages were directly calibrated in pounds of force and required no corrections. The normal-force and pitching-moment gages were also calibrated in pounds and foot pounds, respectively, but it was necessary to correct these readings for torque reactions in the fan drive gear box. The torque reactions were computed from the power input data and were subtracted from the values indicated by the strain gages.

Accuracy of Measuring Devices

The various measuring devices used were accurate within the following limits. The values given include error limits involved in reading and reducing the data as well as the accuracy of the device itself.

Duct angle	$\pm 0.2^{\circ}$
Lift	±10 lb
Drag	±2 lb
Pitching moment	±30 ft-lb
Fan rotational speed	±0.5 rps
Shaft horsepower	±20
Free-stream dynamic pressure	±0.2 lb/sq ft

RESULTS AND DISCUSSION

Basic Aerodynamic Characteristics

Ducted fan.- Two basic types of coefficients have been used to define the aerodynamic characteristics of the ducted fan. The first type is referred to the wind axis and is based on the free-stream dynamic pressure and the product of duct chord and duct exit diameter. The second type is referred to the duct thrust axis and is based on the fan rotational speed and fan diameter. The results of tests of the ducted fan at angles of attack from 0° to 90° defined by the first type of coefficient are shown in figure 4 and by the second type in figure 5. These tests were all conducted with the wing in place at 0° angle of attack, and with a fan-blade angle of 15° at the tip.

The propulsive performance and static efficiency were determined for the ducted fan operating at 0° inclination to the air stream for fan-blade angles of 15° and 23°. The thrust coefficient, power coefficient, and propulsive efficiency are shown as functions of advance ratio in figure 6. The static performance is defined in figure 7 by the thrust to horsepower ratio and the fan tip speed which are shown as functions of the disc loading. The maximum propulsive efficiency shown in figure 6 is about 62 percent whereas the data of reference 5 indicate that maximum efficiencies in excess of 80 percent could reasonably be expected with proper design. Similarly, the maximum[1] figure of merit, determined from figure 7 by means of the expression

$$\text{figure of merit} = \frac{\text{thrust}^{3/2}}{\text{SHP}47.5d_e}$$

(about 74 percent at a blade angle of 23°), was less than the value of about 80 percent obtained from the data of reference 5.

Wing and ducted fan.- The aerodynamic characteristics of the wing alone are shown in figure 8 and the characteristics of the wing and ducted fan together, in figure 9. These coefficients are based on the free-stream dynamic pressure and the wing geometry and are referred to the wind axis, with advance ratio and wing angle as the independent parameters.

Stall Boundary for Upstream Duct Lip

The results of figures 4(b), 5(b), and 9(b) indicate that at large duct angles of attack, the pitching-moment coefficients reached a maximum value and then decreased. In addition, the normal-force coefficient

[1]Figure of merit did not vary with disc loading for the range examined.

versus power coefficient, results of figure 5(b), indicates that a sharp increase in power coefficient also occurred at these same conditions. Tuft studies showed that these characteristics were caused by stalling of the inside of the upstream duct lip. In addition, this lip stall was accompanied by a sudden increase in the noise level, which suggested an asymmetric loading on the fan. The onset of this stall was considered to have begun when the rate of change of the pitching-moment coefficient with respect to the duct angle of attack $dC_m/d\alpha_d$ began to decrease rapidly, as indicated in figures 4(b) and 5(b) by small crosses on the pitching-moment coefficient curves.[2] From these results, figure 10(a) was developed which shows the duct angle of attack at which the duct lip stall occurred as a function of the advance ratio.

To evaluate the significance of this lip stall boundary, the duct angle and advance ratio requirements of the vehicle of reference 1 for low-speed, level, unaccelerated flight were determined from figure 9(a).[3] The advance ratio was then used to determine the duct-lip stall boundary from figure 10(a). The results are shown in figure 10(b) where the duct-lip stall boundary and the variation of the duct angle required for level, unaccelerated flight are compared. These results indicate that at 0° wing angle of attack there is always a duct angle of attack margin of at least 8°.

Vertical Velocity Limitation

The vertical velocity which can be attained by a vehicle employing wing-tip-mounted ducted fans can be limited by duct lip stall, wing stall, or power. Only the limitations due to duct lip stall will be considered here. To gain some insight into the effects of duct lip stall on the vertical velocity, curves of constant vertical velocity for the vehicle of reference 1 in unaccelerated flight were superimposed upon the faired C_L vs. C_D curves of figures 9 as illustrated for 0° wing angle of attack in figure 11(a). Negative vertical velocity represents descending flight and positive velocity represents climb. The indicated lip stall boundaries have been taken from figure 10(a). It is apparent from this figure that duct lip stall would limit the maximum descent velocity but not the climb velocity. The descent boundary curves are shown in figure 11(b), where descent velocity is presented as a function of horizontal velocity for wing angles of attack of 0°, 4°, 8°, and 12°.

---

[2]Most of the curves stopped at, or slightly past, the onset of lip stall because there was no means of monitoring the fan-blade stresses and, hence, of knowing the magnitude of the fan-blade stresses due to the suspected asymmetric fan loading.

[3]The physical conditions assumed were a semispan lift of 1550 pounds and a semispan drag of 0.96 times the dynamic pressure in psf.

These results indicate that for 0° wing angle of attack, allowable descent velocities, without encountering lip stall, ranged from about 370 fpm for a horizontal velocity of 30 knots to about 2100 fpm for 75 knots. Increasing the wing angle of attack increased the allowable descent rates since for a given descent rate, the wing lift and drag made it possible to operate the duct at a lower angle of attack. It should be noted that any device that would increase the wing effectiveness, such as a trailing-edge flap or leading-edge droop, would also increase the allowable descent rates (see ref. 2).

Effect of the Wing on Power Required During Transition

To evaluate this effect the power required for transition from hover to 80 knots for the vehicle of reference 1 was examined for various wing attitudes. The results are shown in figure 12, where the shaft horsepower is presented as a function of the forward velocity for wing angles of attack of 0°, 4°, 8°, and 12°. The power required for the ducted fan alone is presented also. From this figure it is evident that less power was required when the wing angle of attack was increased, as was shown in reference 3. However, it must be noted that the rate of decrease is less for wing angles greater than 4°, probably because of the occurrence of local separation on the wing at the wing-duct juncture, as was indicated in reference 2.

Ames Research Center
National Aeronautics and Space Administration
Moffett Field, Calif., Feb. 1, 1962

REFERENCES

1. Yaggy, Paul F., and Mort, Kenneth W.: A Wind-Tunnel Investigation of a 4-Foot-Diameter Ducted Fan Mounted on the Tip of a Semispan Wing. NASA TN D-776, 1961.

2. Yaggy, Paul F., and Goodson, Kenneth W.: Aerodynamics of a Tilting Ducted Fan Configuration. NASA TN D-785, 1961.

3. Goodson, Kenneth W., and Grunwald, Kalman J.: Aerodynamic Characteristics of a Powered Semispan Tilting-Shrouded-Propeller VTOL Model in Hovering and Transition Flight. NASA TN D-981, 1961.

4. Grunwald, Kalman J., and Goodson, Kenneth W.: Aerodynamic Loads on an Isolated Shrouded-Propeller Configuration for Angles of Attack from -10° to 110°. NASA TN D-995, 1961.

5. Grose, Ronald M.: Wind Tunnel Tests of Shrouded Propellers at Mach Numbers From 0 to 0.60. WADC TR 58-604, United Aircraft Corporation, 1958.

TABLE I.- BASIC DIMENSIONS OF DUCTED FAN AND WING

Duct	
Inside diameter, ft	4
Outside diameter	4 ft 10.5 in.
Chord	2 ft 9 in.
Exit diameter	4 ft 6.3 in.
Diffuser angle, deg	11
Inlet guide vanes	
Chord, in.	3
Number of vanes	7
Airfoil section	NACA 65A010
Position of vane c/4, percent of duct chord	12.1
Twist, deg	0
Fan	
Plan-form curves	(see fig. 3)
Number of blades	8
Hub to tip diameter ratio	0.333
Position of hub center line, percent of duct chord	29.3
Design static thrust disc loading, psf	150
Design static power disc loading, HP/ft^2	7.96
Blade angle control	fixed pitch
Blade angle at tip, deg	15 and 23
Stators	
Number of stators	9
Position of stator c/4, percent of duct chord	49.4
Twist, center body to tip, deg	15
Airfoil shape	(see text)
Wing	
Airfoil section	NACA 2418
Area, ft^2	48
Semispan, ft	8
Mean aerodynamic chord, ft	6.09
Taper ratio	0.675

TABLE II.- SHROUD AND CENTERBODY COORDINATES

Shroud coordinates tabulated in percent of shroud chord (33.00 in.)			Centerbody coordinates tabulated in percent of centerbody length (71.5 in.)	
Chordwise length, X	Outside radius, r_o	Inside radius, r_i	Length, X	Radius, r
0	81.5	81.5	0	0
.5	83.4	79.6	.5	2.07
.75	83.8	79.0	1.25	3.20
1.25	84.4	78.4	2.50	4.46
2.5	85.4	77.2	5.0	6.17
5.0	86.4	75.8	7.5	7.40
7.5	87.1	74.9	10.0	8.31
10.0	87.6	74.2	15.0	9.68
15.0	88.2	73.3	20.0	10.54
20.0	88.6	72.9	25.0	11.01
25.0	88.6	72.7	25.875[1]	11.06
30.0	88.6	72.7	30.0	11.19
35.0	88.6	72.7	32.57[2]	11.19
40.0	88.6	72.7	40.0	11.19
45.0	88.6	72.7	50.0	11.19
50.0	88.6	72.7	60.0	11.19
55.0	88.6	73.2	70.0	10.49
60.0	88.6	74.1	72.05[3]	10.14
65.0	88.0	75.1	80.0	7.97
70.0	87.4	76.1	83.20	6.77
75.0	86.8	77.1	90.0	4.03
80.0	85.9	78.1	95.0	2.01
85.0	85.2	79.1	100.0	0
90.0	84.3	80.1		
95.0	83.3	81.1		
100.0	82.2	82.0		

[1]Shroud leading-edge position.
[2]Inlet guide vane c/4 line position.
[3]Shroud trailing-edge position.

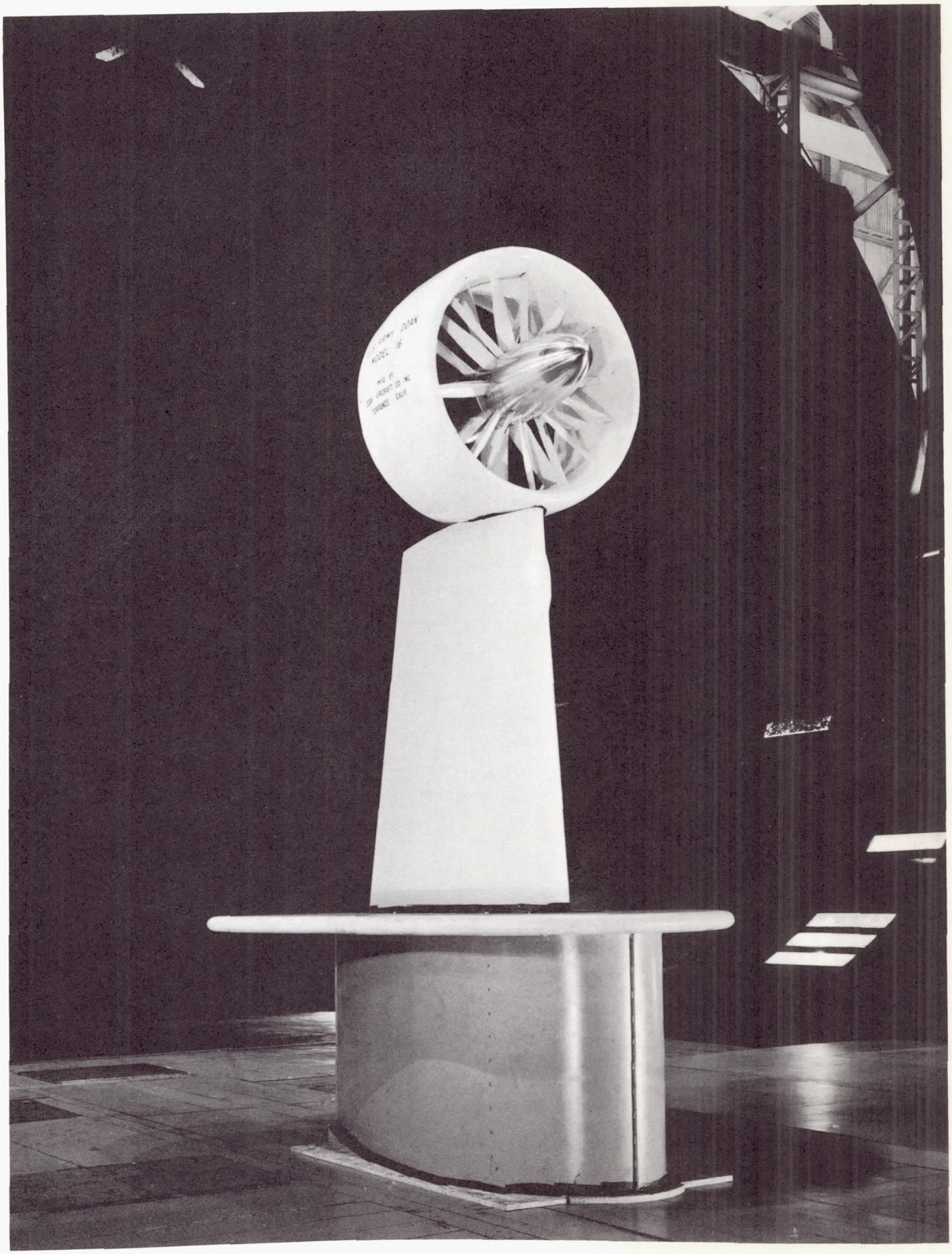

A-25140.1

Figure 1.- Ducted fan model mounted in the Ames 40- by 80-Foot Wind Tunnel.

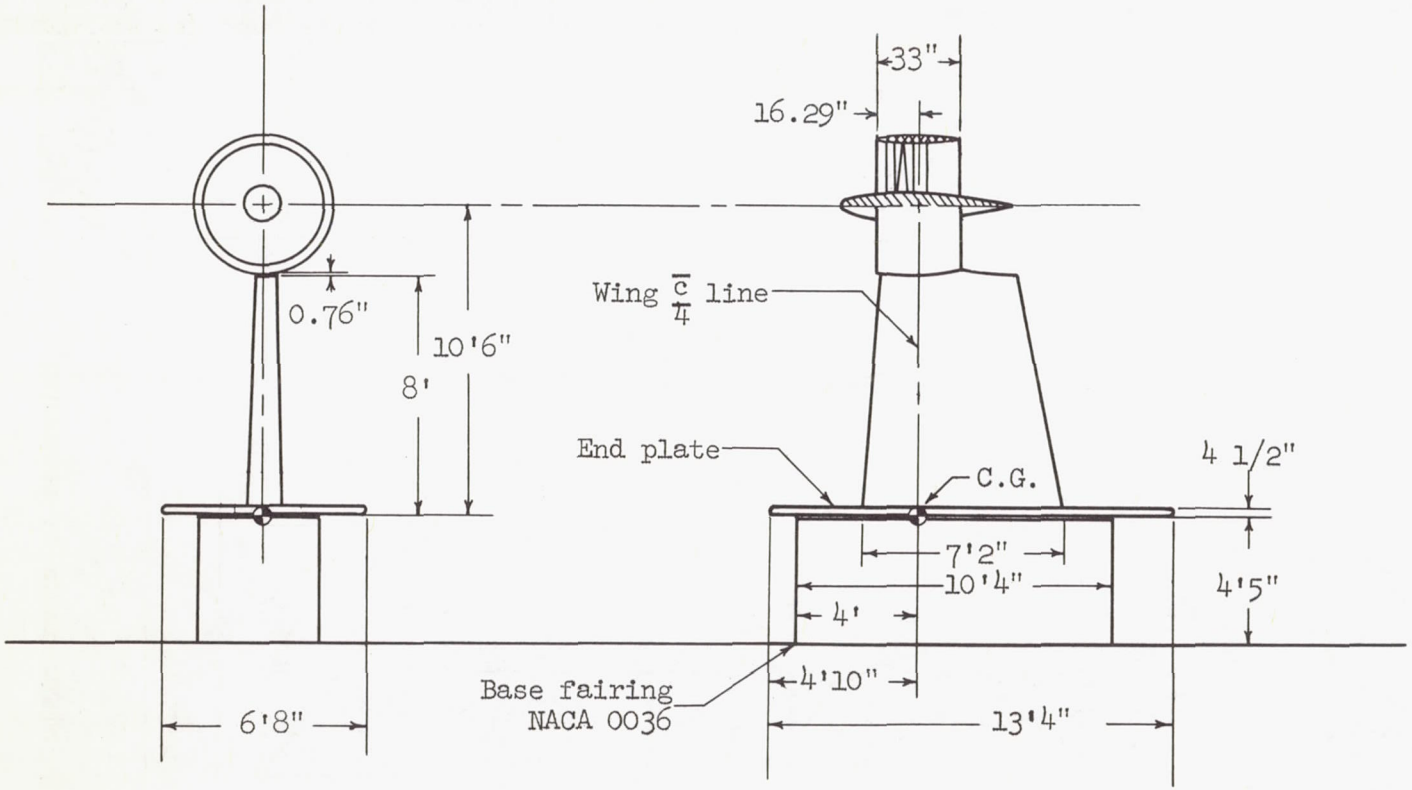

Figure 2.- Basic model dimensions.

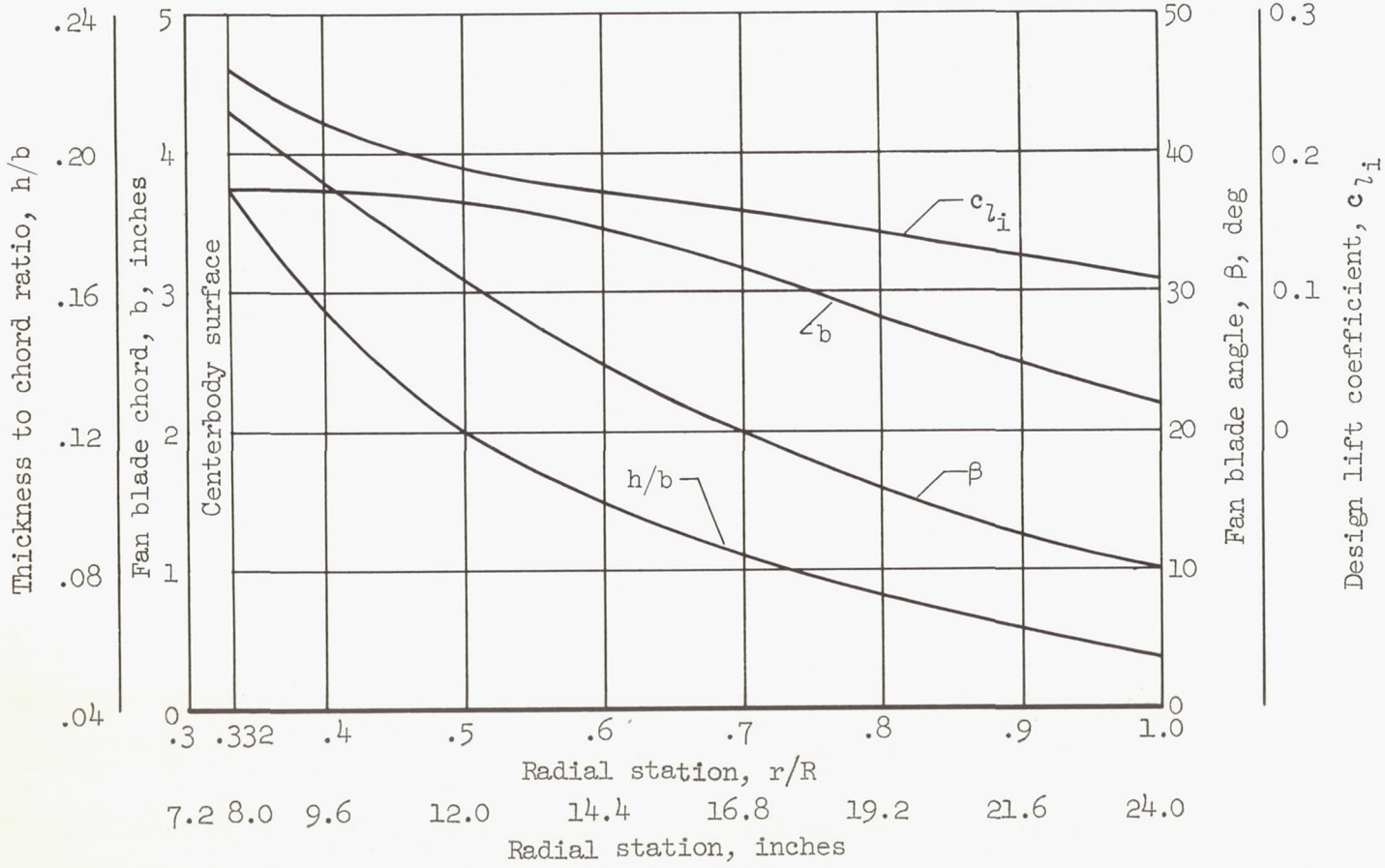

Figure 3.- Fan blade-form curves with the design lift coefficient, blade chord, blade angle, and blade thickness to chord ratio as functions of the radial distance from the duct center.

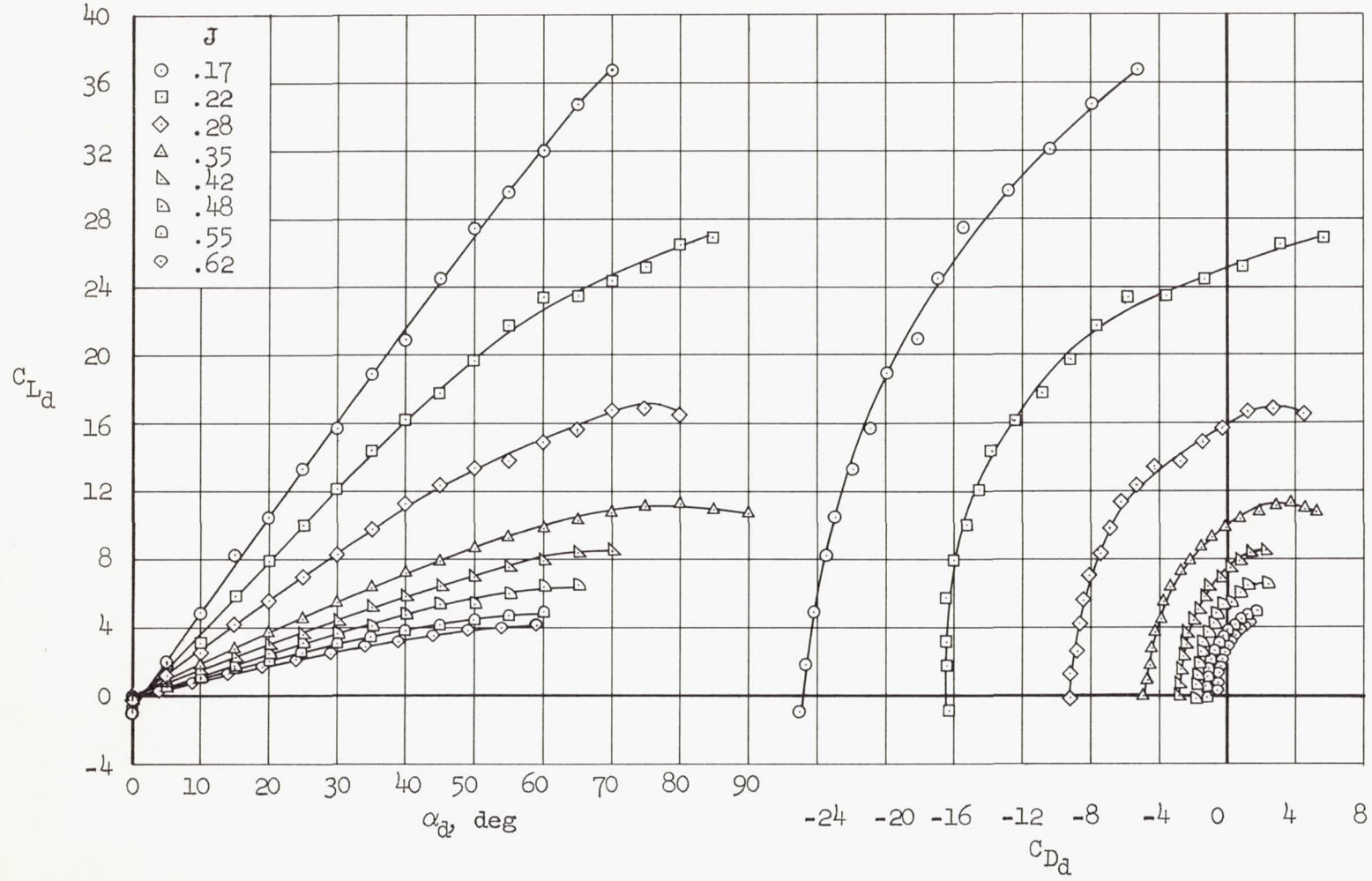

(a) Lift coefficient as a function of duct angle of attack and drag coefficient.

Figure 4.- Aerodynamic characteristics of the ducted fan with the coefficients based on duct geometry and free-stream dynamic pressure for several advance ratios; $\beta = 15^{\circ}$, $\alpha_w = 0^{\circ}$.

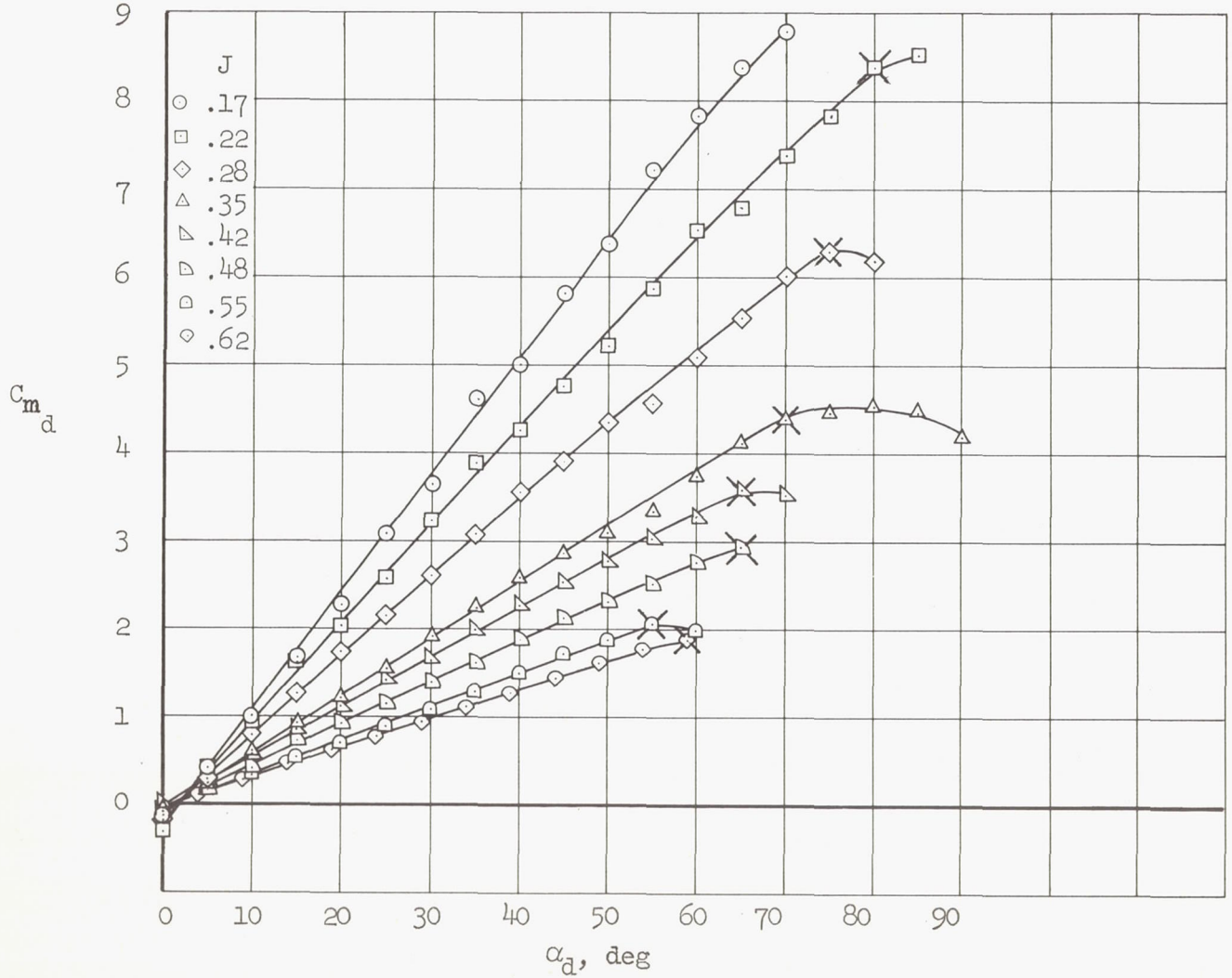

(b) Pitching-moment coefficient as a function of duct angle of attack.

Figure 4.- Concluded.

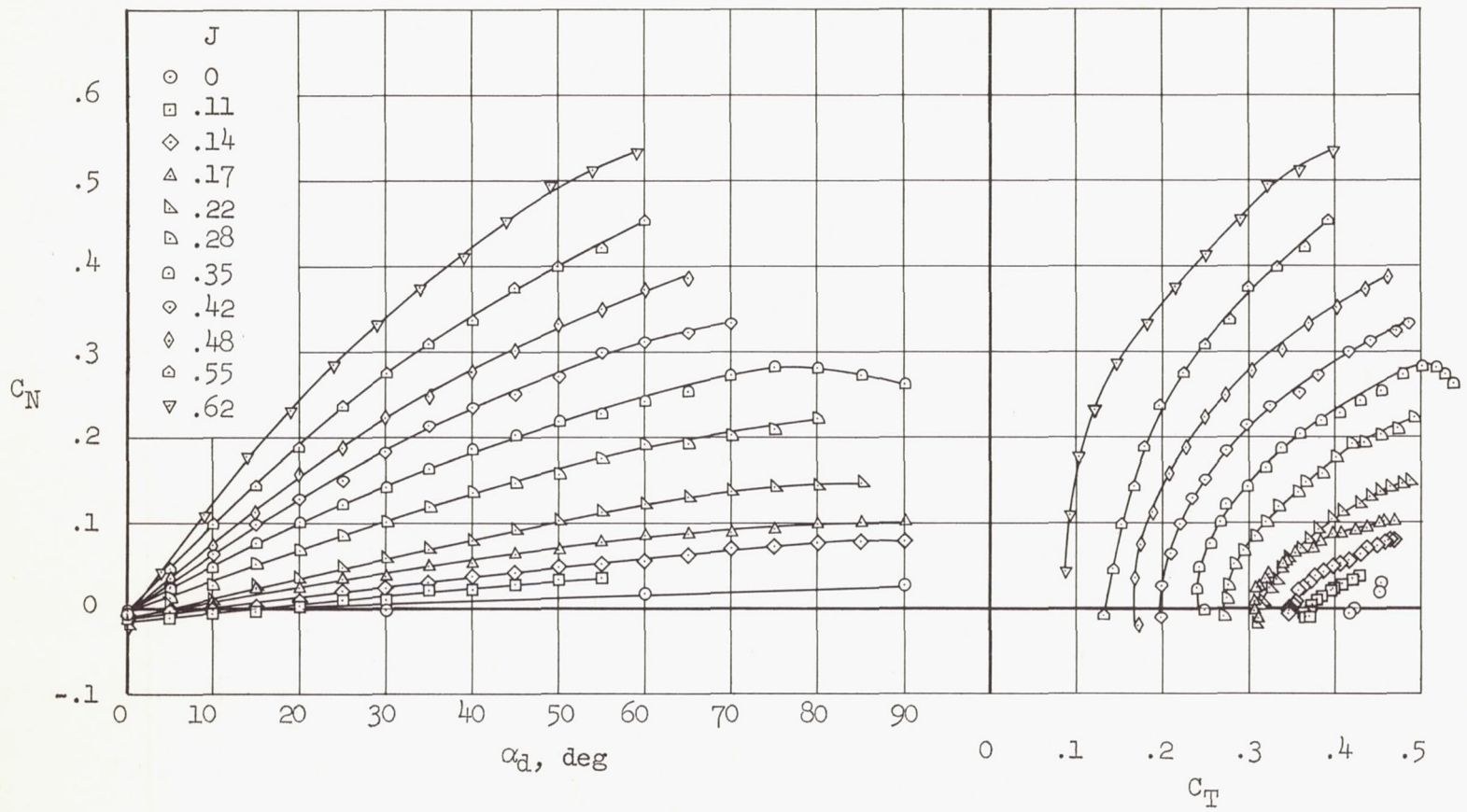

(a) Normal-force coefficient as a function of duct angle of attack and thrust coefficient.

Figure 5.- Aerodynamic characteristics of the ducted fan with the coefficients based on fan diameter and rotational speed for several advance ratios; $\beta = 15^\circ$, $\alpha_w = 0^\circ$.

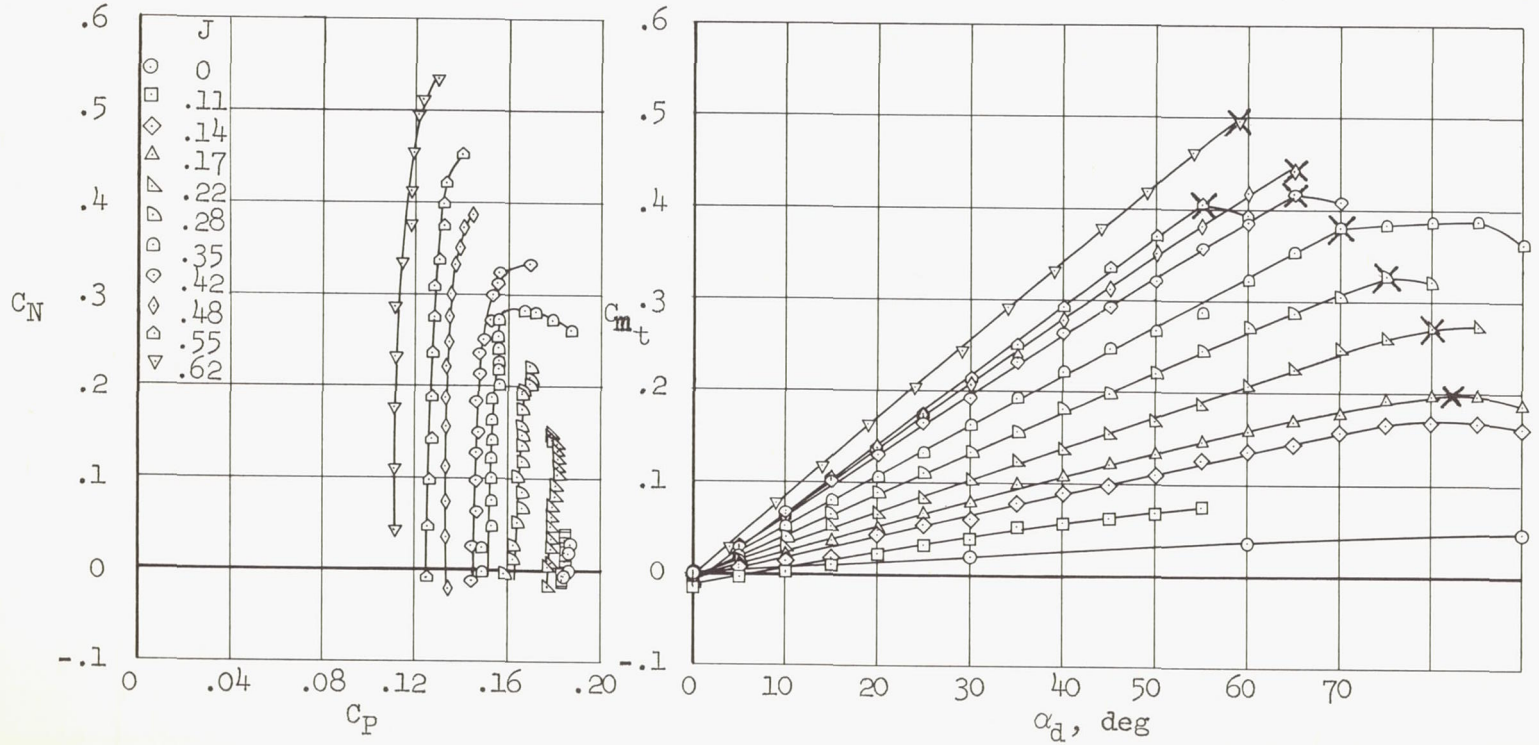

(b) Normal-force coefficient as a function of power coefficient and pitching-moment coefficient as a function of duct angle of attack.

Figure 5.- Concluded.

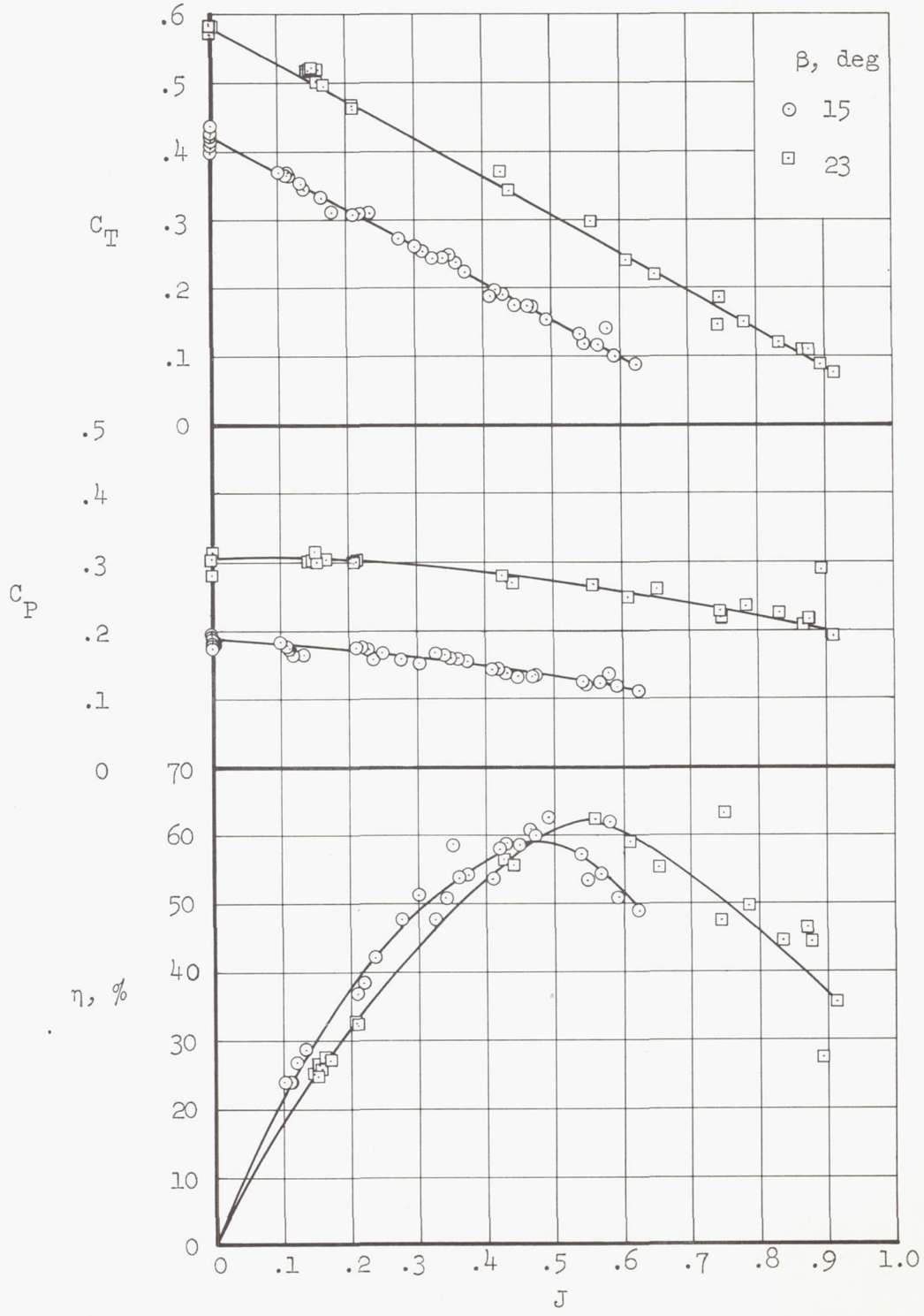

Figure 6.- Thrust coefficient, power coefficient, and propulsive efficiency as functions of advance ratio for 0° duct angle of attack.

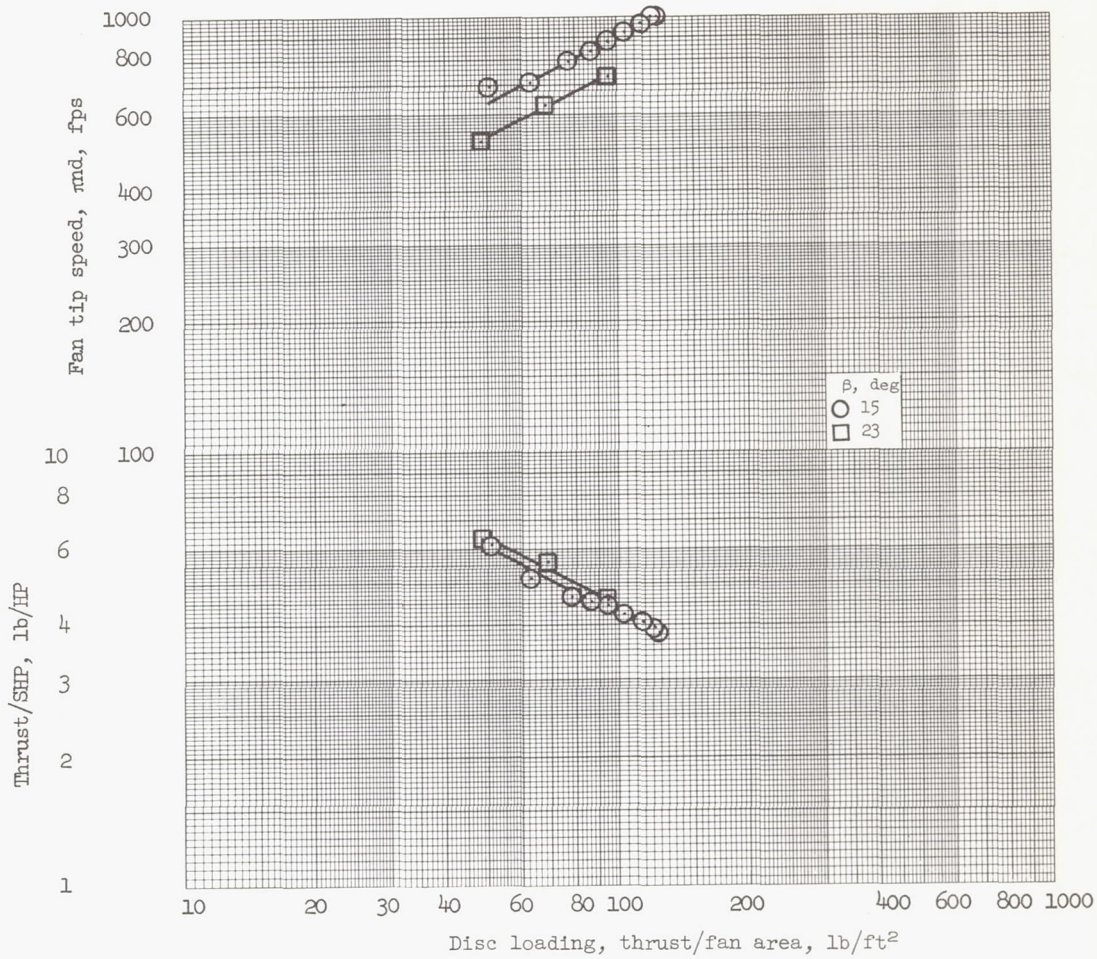

Figure 7.- Thrust to horsepower ratio and tip speed as functions of fan disc loading for zero forward velocity.

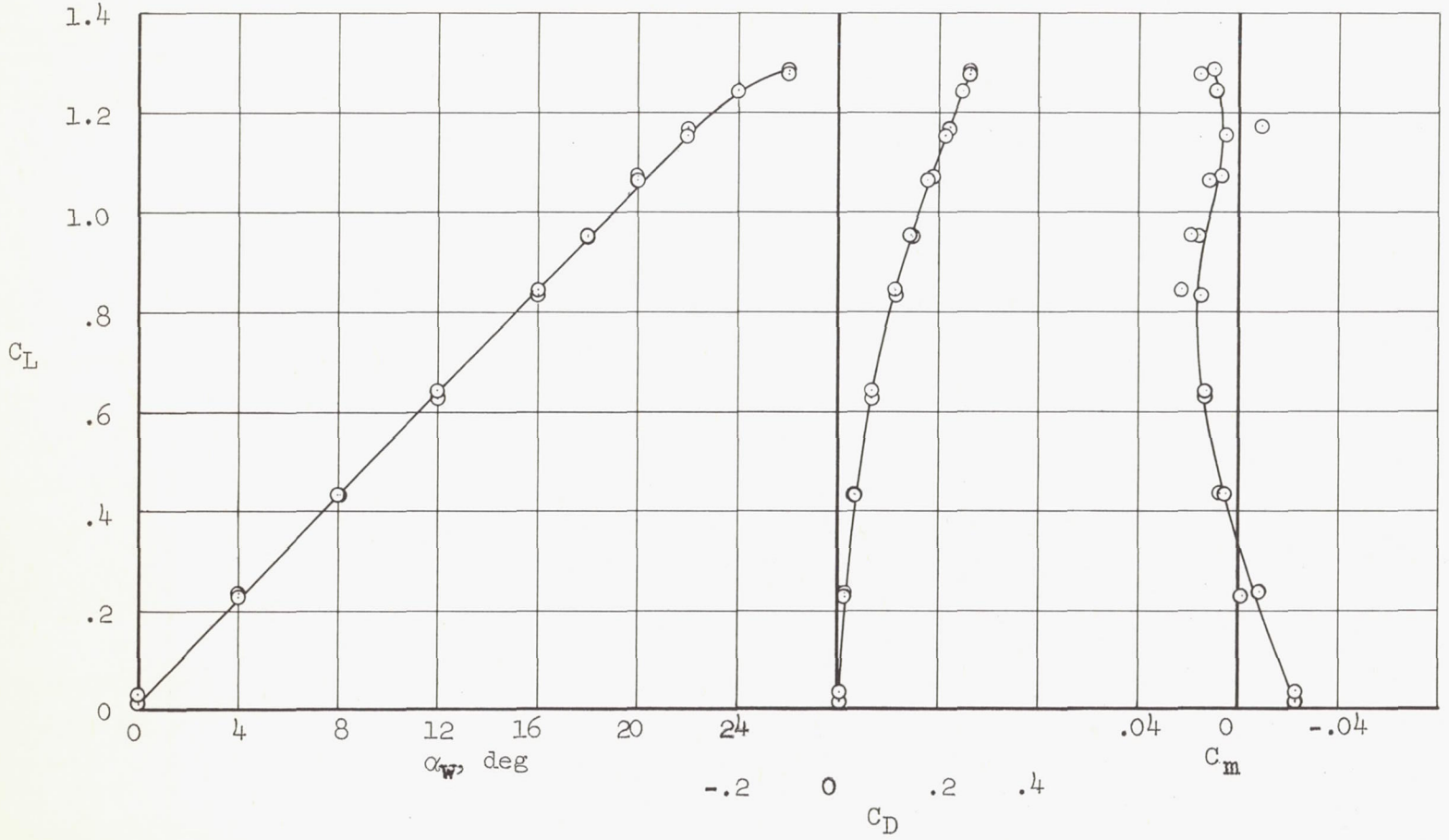

Figure 8.- Aerodynamic characteristics of the wing alone.

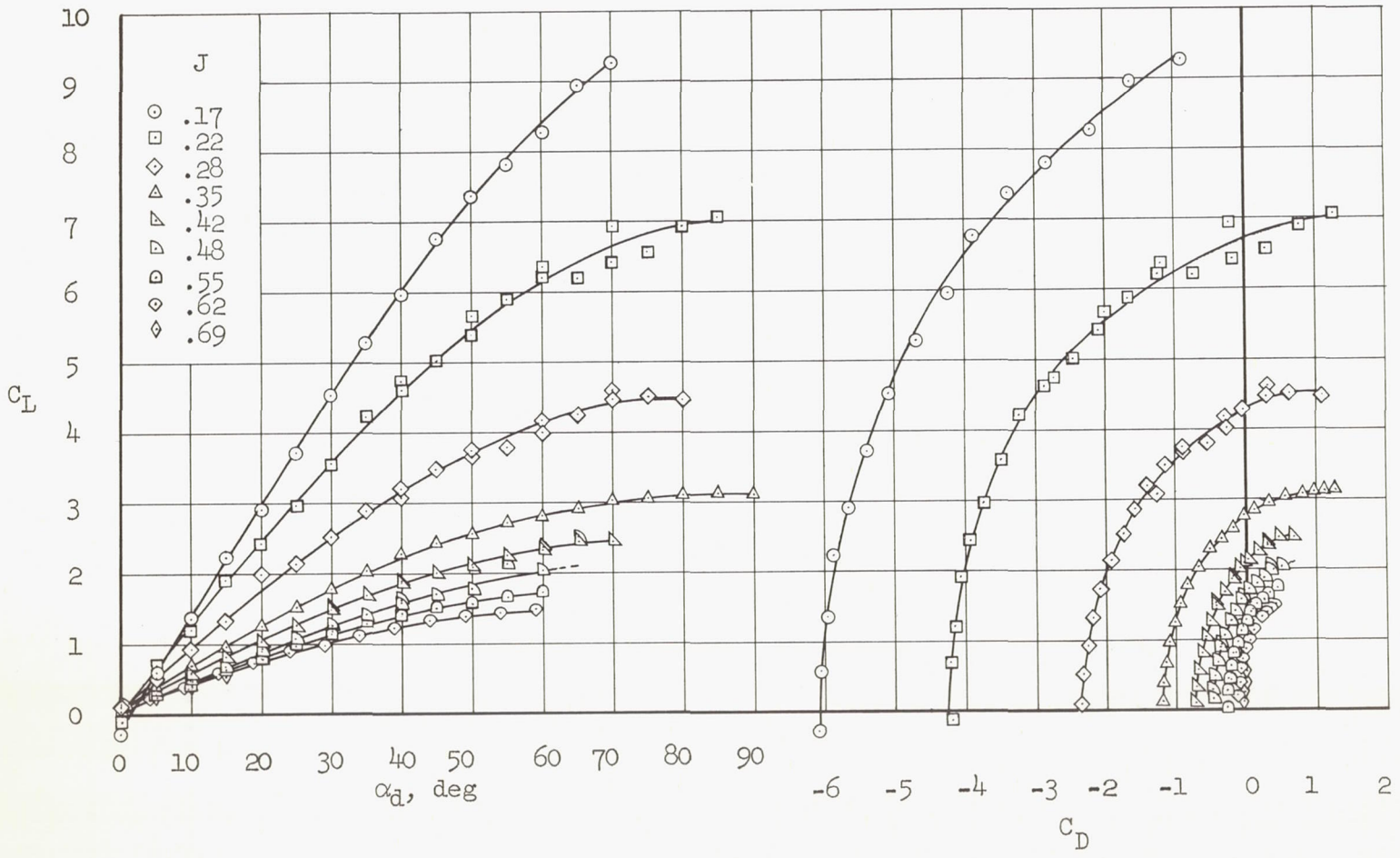

(a) $\alpha_w = 0^\circ$

Figure 9.- Aerodynamic characteristics of the wing and ducted fan with the coefficients based on wing area and free-stream dynamic pressure for several advance ratios, and at four wing angles of attack; $\beta = 15^\circ$.

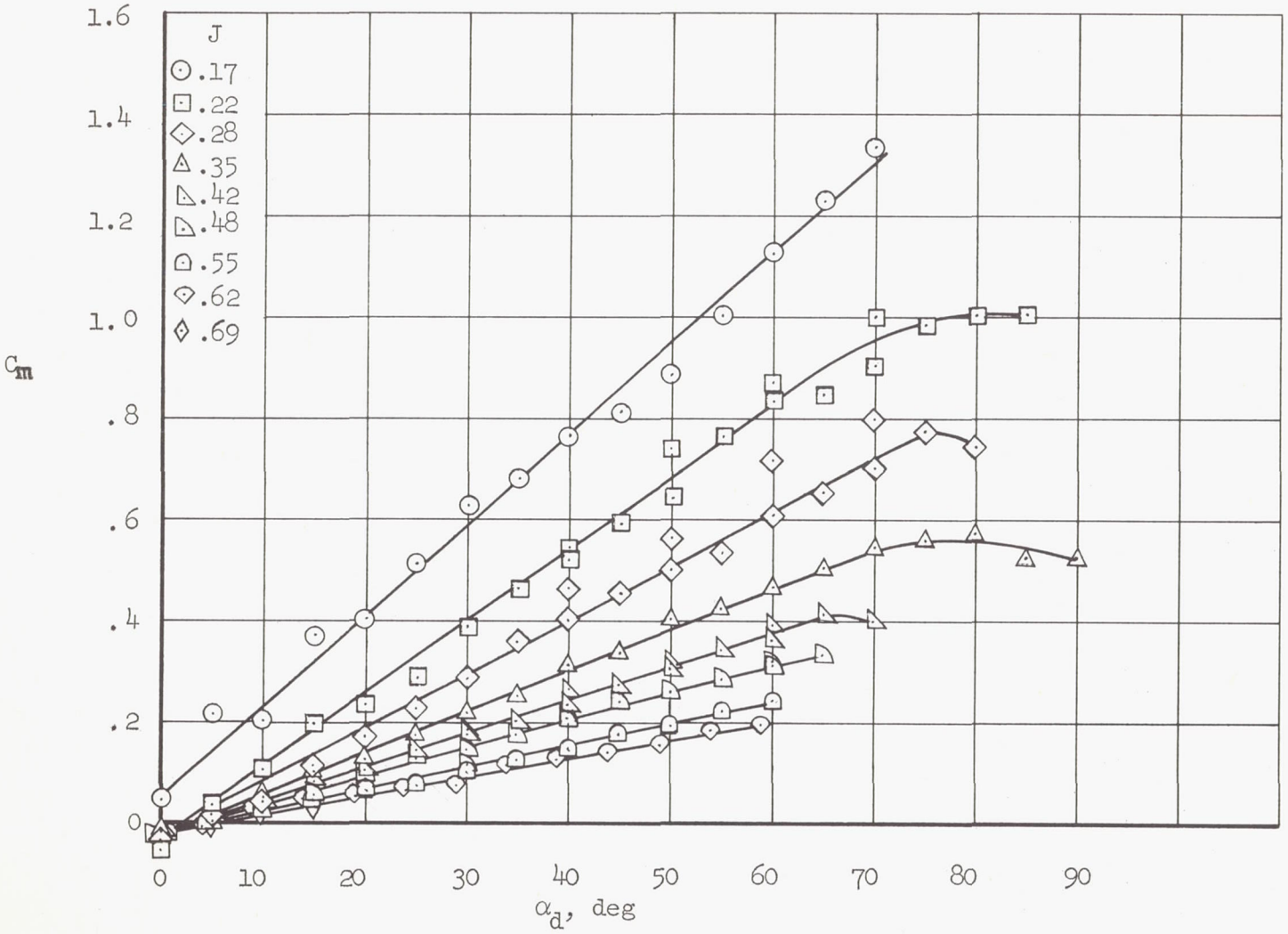

(b) $\alpha_w = 0^\circ$

Figure 9.- Continued.

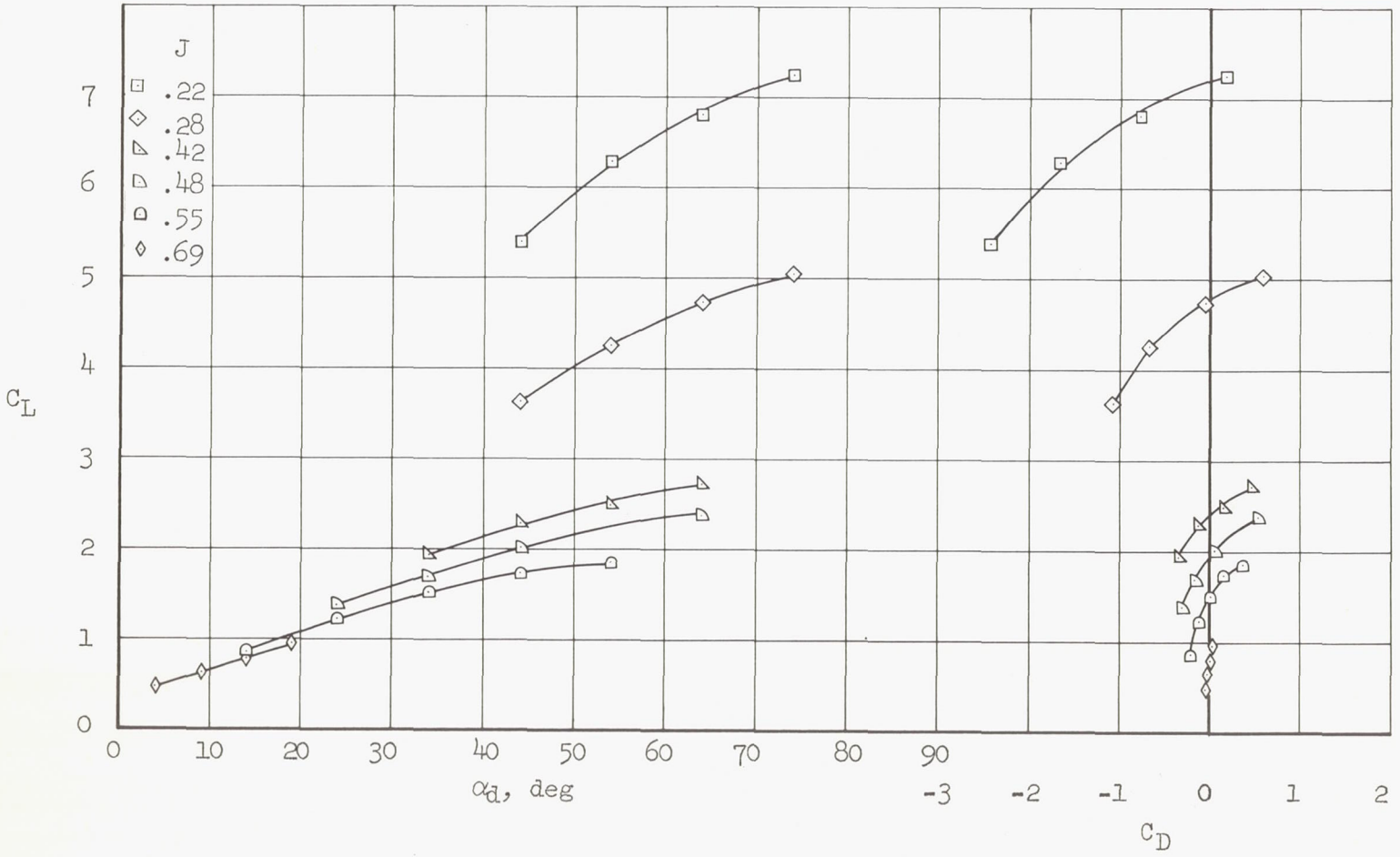

(c) $\alpha_W = 4^\circ$

Figure 9.- Continued.

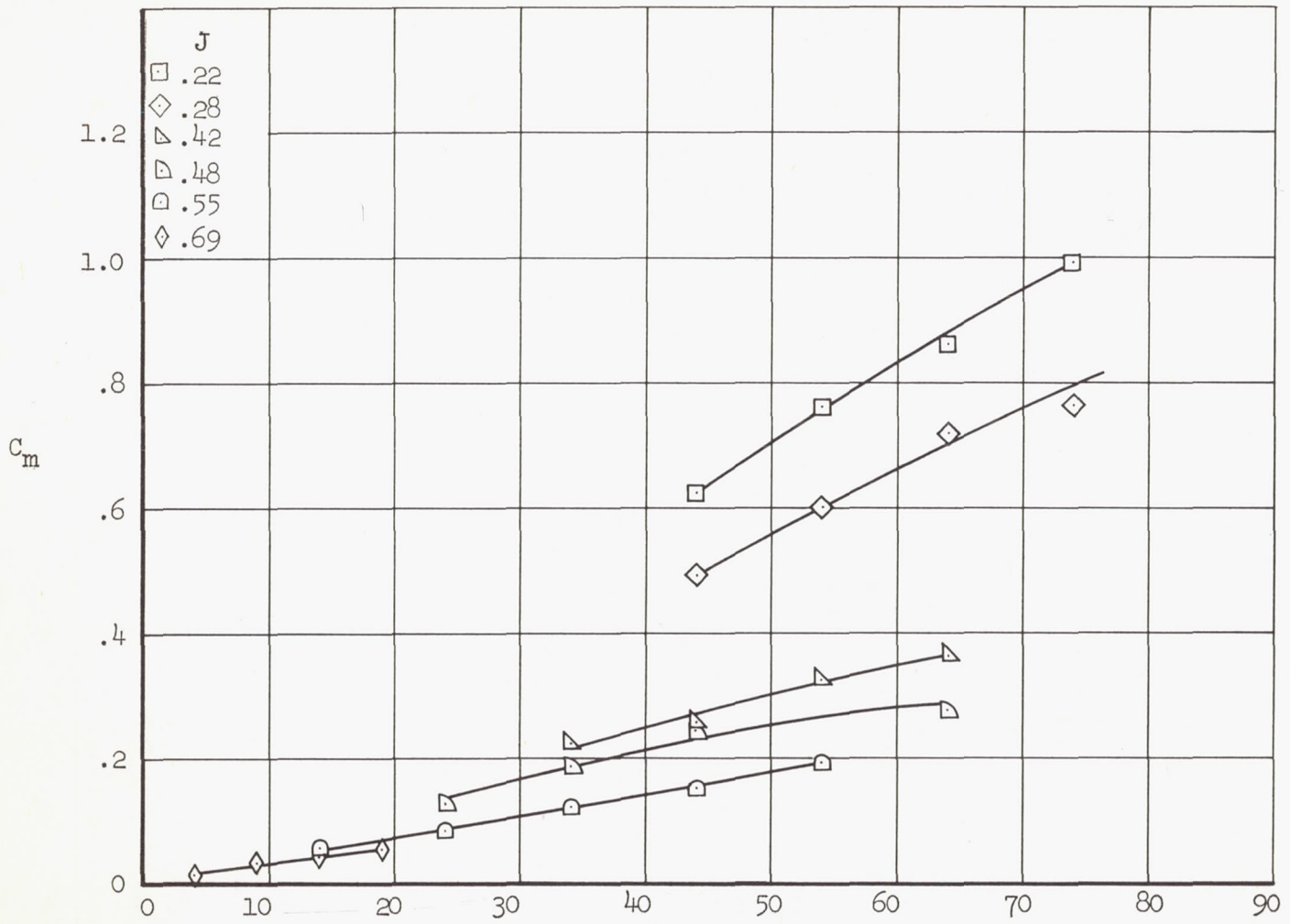

(d) $\alpha_w = 4^\circ$

Figure 9.- Continued.

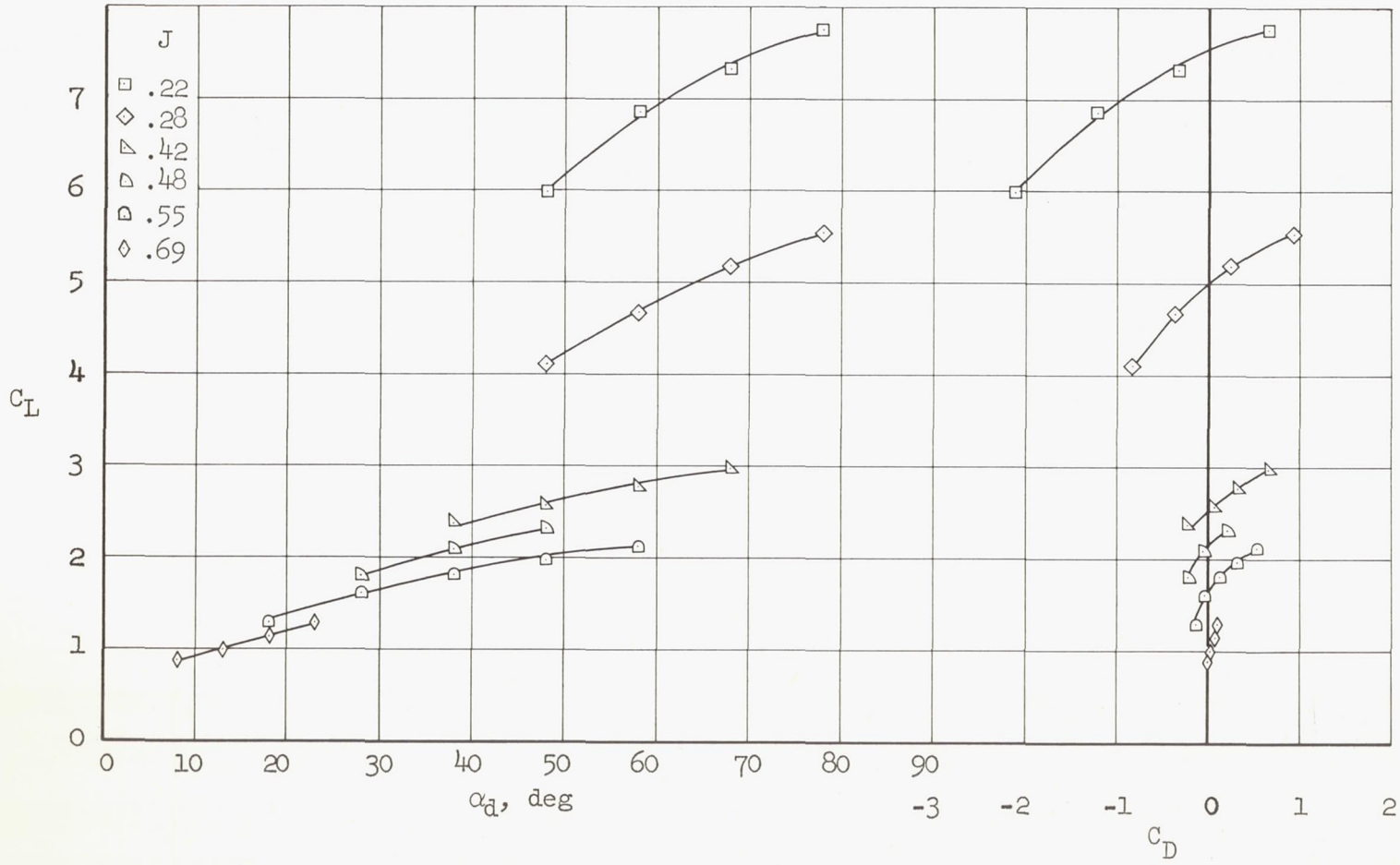

(e) $\alpha_w = 8^\circ$

Figure 9.- Continued.

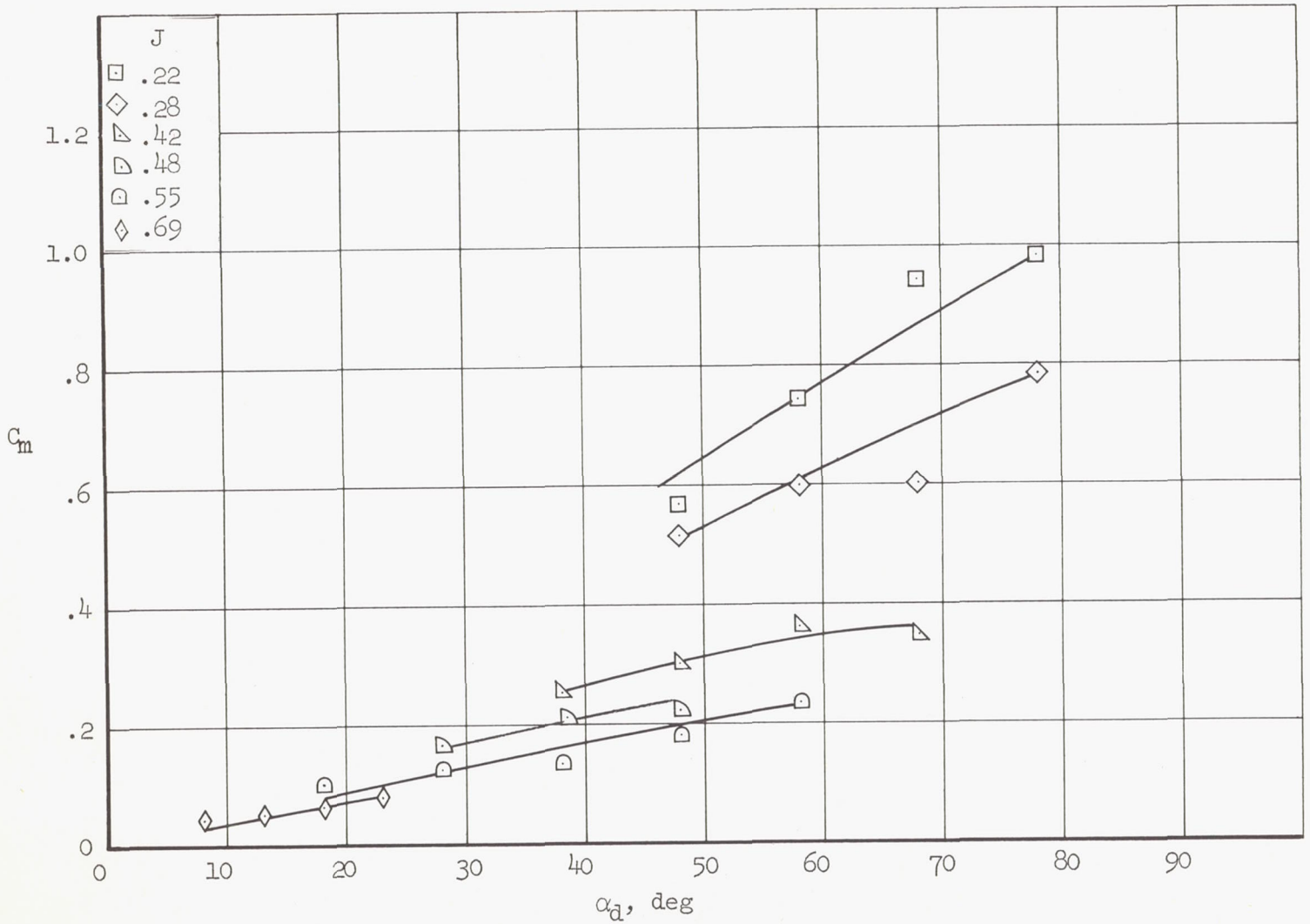

(f) $\alpha_w = 8^\circ$

Figure 9.- Continued.

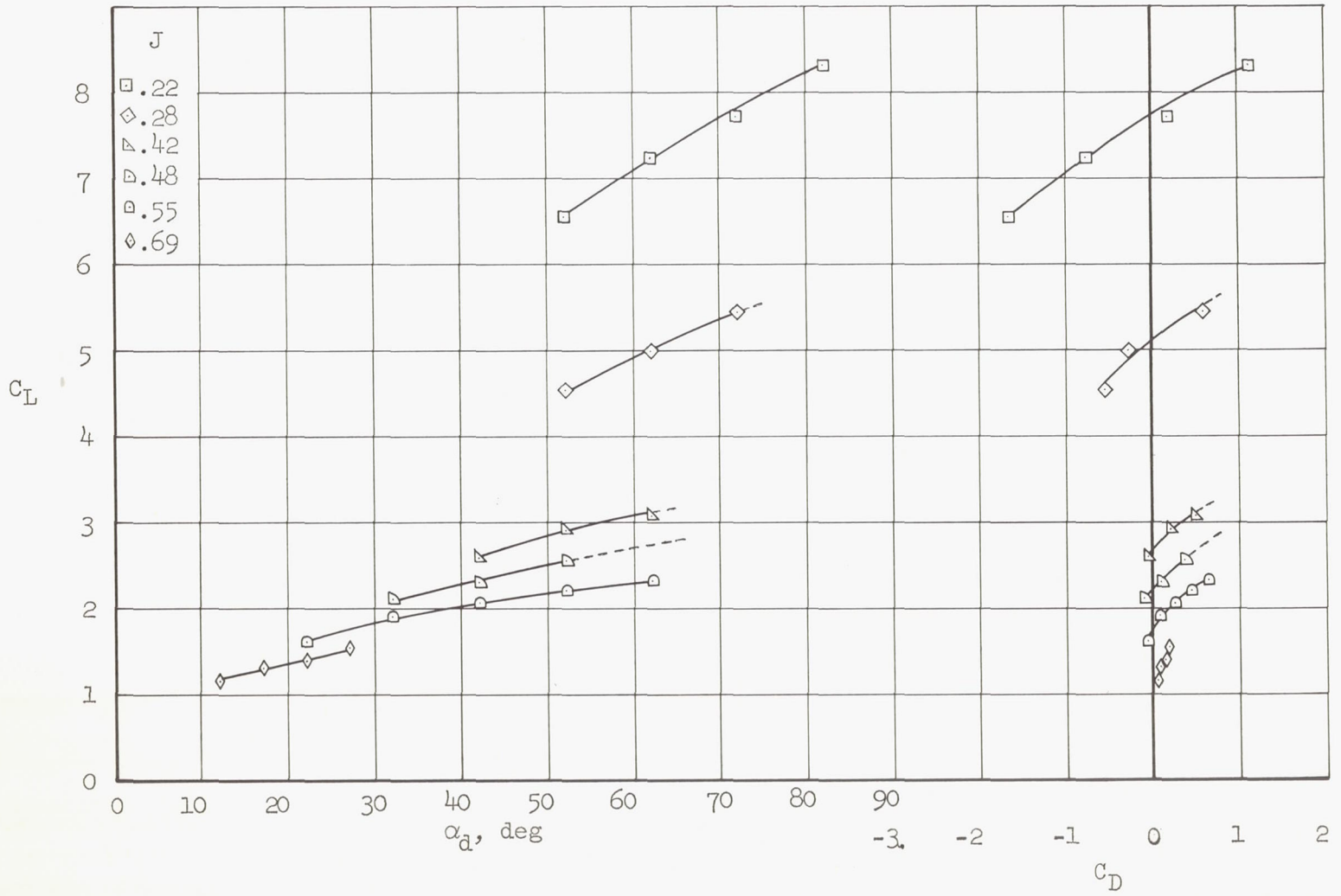

(g) $\alpha_w = 12^\circ$

Figure 9.- Continued.

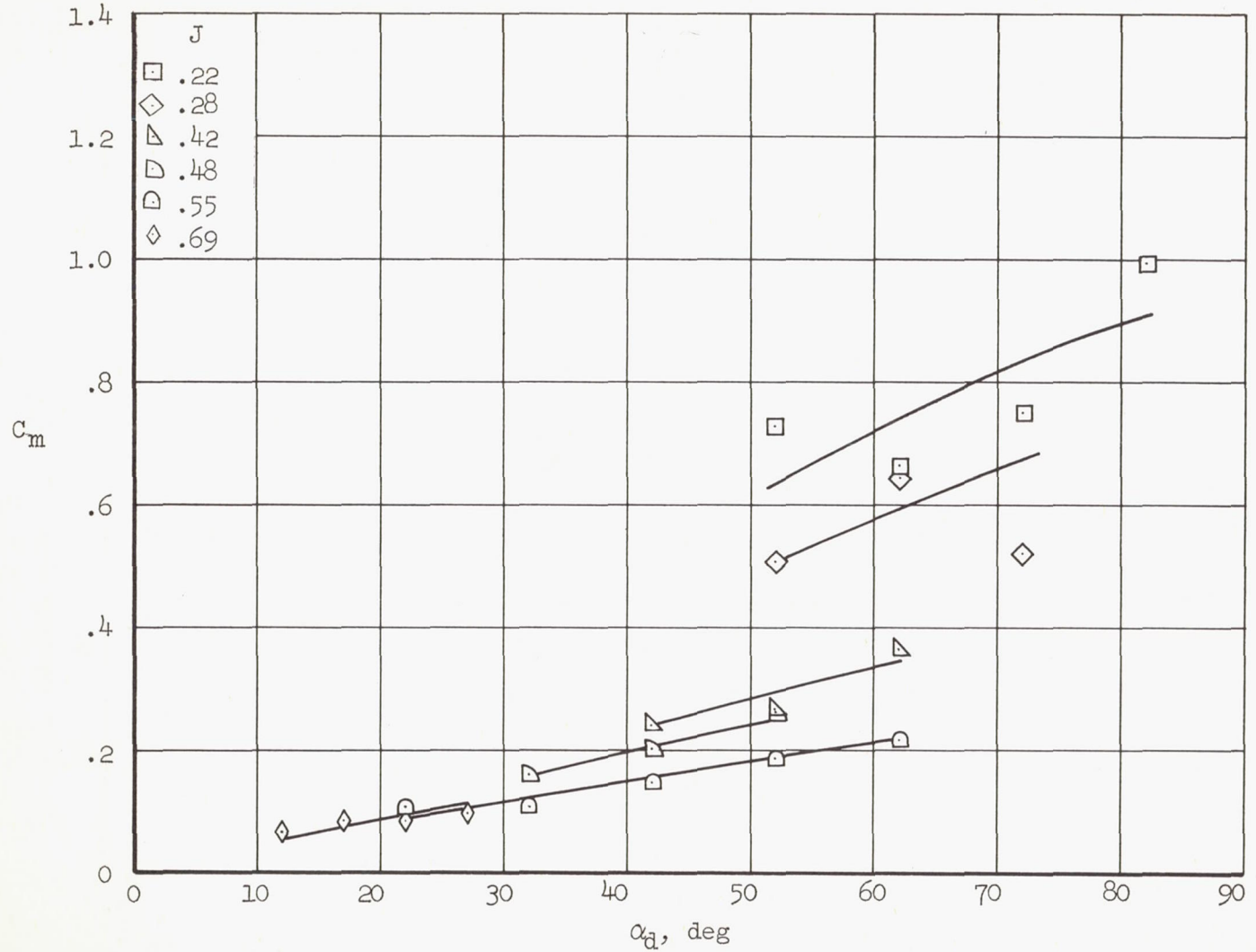

(h) $\alpha_w = 12^\circ$

Figure 9.- Concluded.

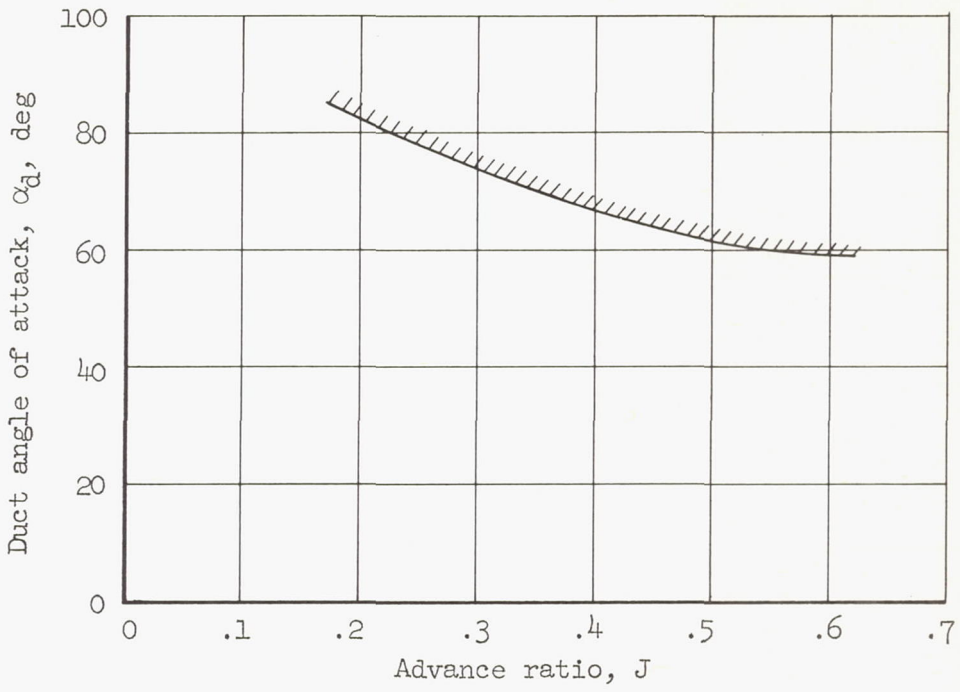

(a) Duct-lip stall boundary as a function of advance ratio.

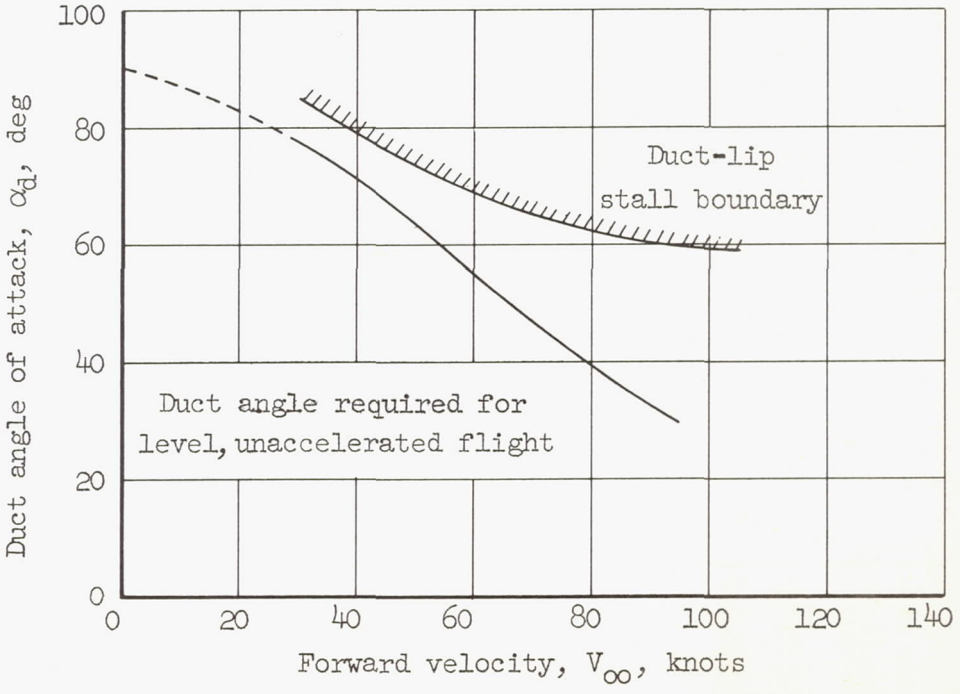

(b) Duct angle of attack as a function of forward velocity.

Figure 10.- Definition of upstream duct-lip stall boundary.

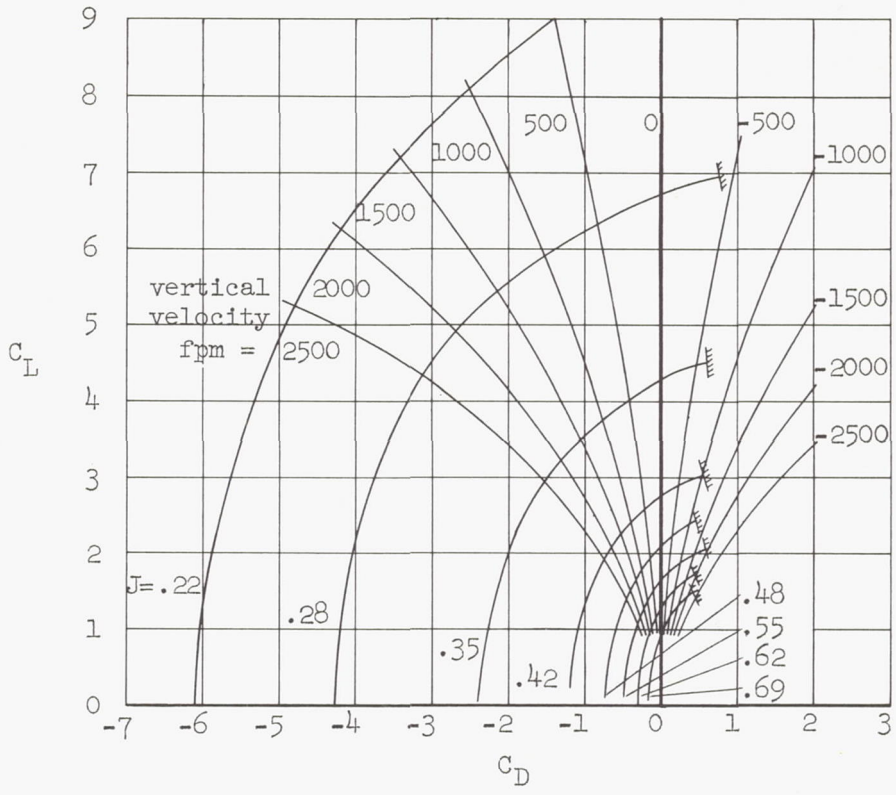

(a) Curves of constant vertical velocity superimposed upon the wing-duct aerodynamic characteristics at $\alpha_w = 0^o$.

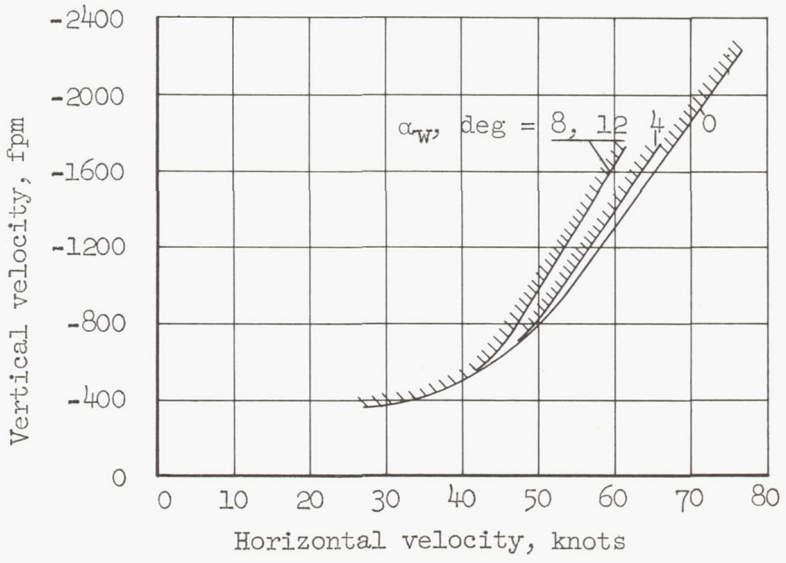

(b) Vertical velocity boundary.

Figure 11.- Definition of vertical velocity boundary due to duct lip stall.

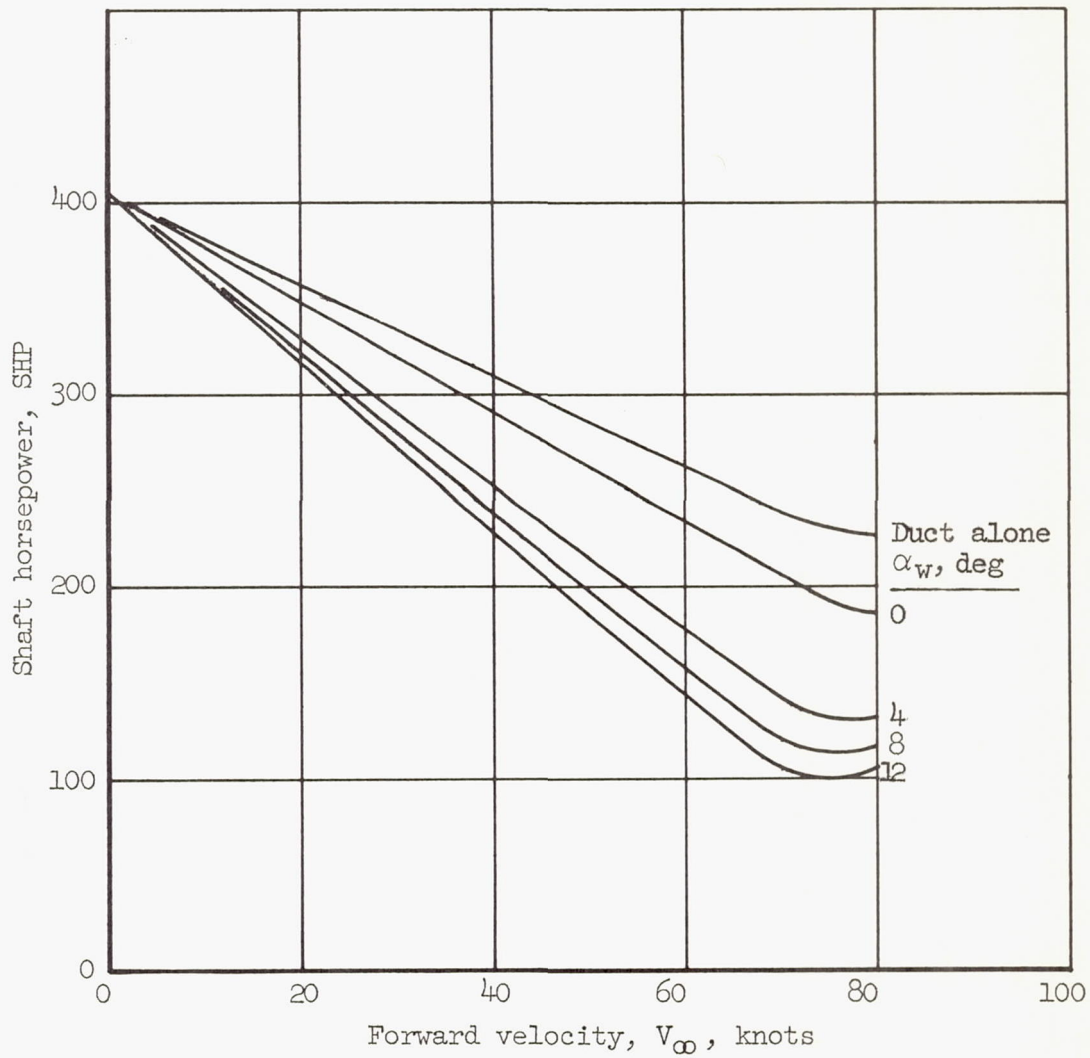

Figure 12.- Effectiveness of the wing in reducing the power required for transition.